Chapter 4

Imaging the Spatial Orientation of Subunits Within Membrane Receptors by Atomic Force Microscopy

Stewart M. Carnally, J. Michael Edwardson, and Nelson P. Barrera

Abstract

Our experimental approach is based on the atomic force microscope (AFM) imaging of epitope-tagged subunits within membrane protein complexes purified in small amounts and decorated by anti-tag antibodies. Furthermore, we can produce simultaneous decoration of protein complexes using Fab fragments and IgG antibodies, which, combined with chemical modification of the substrate, allows us to determine the protein orientation across the cell membrane. Here, we describe a detailed protocol for membrane protein purification, AFM data collection, analysis, and interpretation of results. The protocol also covers basic AFM instrument settings and best practices for both observation of membrane protein complexes by AFM and automatic detection of the structures by an in-house algorithm. Once a sufficient number of membrane protein complexes have been visualized by AFM, data acquisition and processing can be completed in approximately 10 min using a scanning surface of 1 μm^2.

Key words: AFM, Molecular architecture, Membrane receptor, Structural biology, Subunit stoichiometry

1. Introduction

Structural studies of membrane proteins have gained the interest of many research groups. Well-known methods such as X-ray crystallography and cryoelectron microscopy have provided valuable information about the molecular architecture of this family of proteins. However, solubilization conditions, heterogeneity, and size of the protein complexes and different subunit compositions frequently hinder their structural characterization (1). As a consequence, new experimental methods are required to tackle this exciting field. Atomic force microscope (AFM) imaging of

Pier Carlo Braga and Davide Ricci (eds.), *Atomic Force Microscopy in Biomedical Research: Methods and Protocols*, Methods in Molecular Biology, vol. 736, DOI 10.1007/978-1-61779-105-5_4, © Springer Science+Business Media, LLC 2011

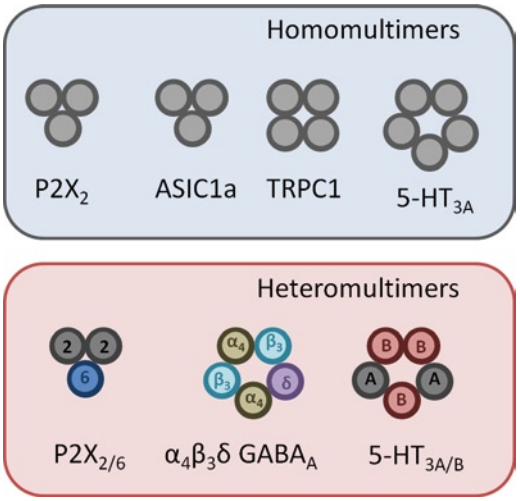

Fig. 1. Scheme showing the molecular architecture of ionotropic receptors and ion channels formed by identical (homomultimers) or different subunits (heteromultimers), identified by AFM imaging of membrane proteins decorated with anti-subunit antibodies.

membrane proteins at single-molecule level has provided valuable insights into receptor–ligand interaction force and structural analysis of subunits and domains (2, 3). However, many receptors expressed at the plasma membrane are functional only as heteromeric entities. In the case of ionotropic receptors in particular, the subunit orientation is key to understanding parameters such as ligand binding, stoichiometry, and ion conductance (4, 5). Furthermore, when subunits within a receptor have similar size and shape, AFM imaging alone cannot detect the subunit spatial orientation. Recently, we have designed a novel approach combining AFM imaging and expression of engineered receptor subunits. This method has led us to propose the molecular architecture of a number of ionotropic receptors and channels that have physiological and therapeutic relevance (Fig. 1) (6–12).

This chapter focuses on the isolation and AFM imaging of intact membrane receptors. This AFM experimental approach is based on the imaging of epitope-tagged subunits within membrane receptors purified in small amounts and decorated by anti-tag antibodies. To reduce possible damage of the isolated proteins by frictional forces, the AFM tapping mode is selected to measure the topography of the samples. An in-house algorithm automatically identifies receptor–antibody complexes and analyzes the molecular volume of their components and the angles of doubly decorated receptor–antibody complexes. This information is then interpreted, in order to deduce the stoichiometry and spatial orientation of subunits within a receptor (Fig. 2). This chapter

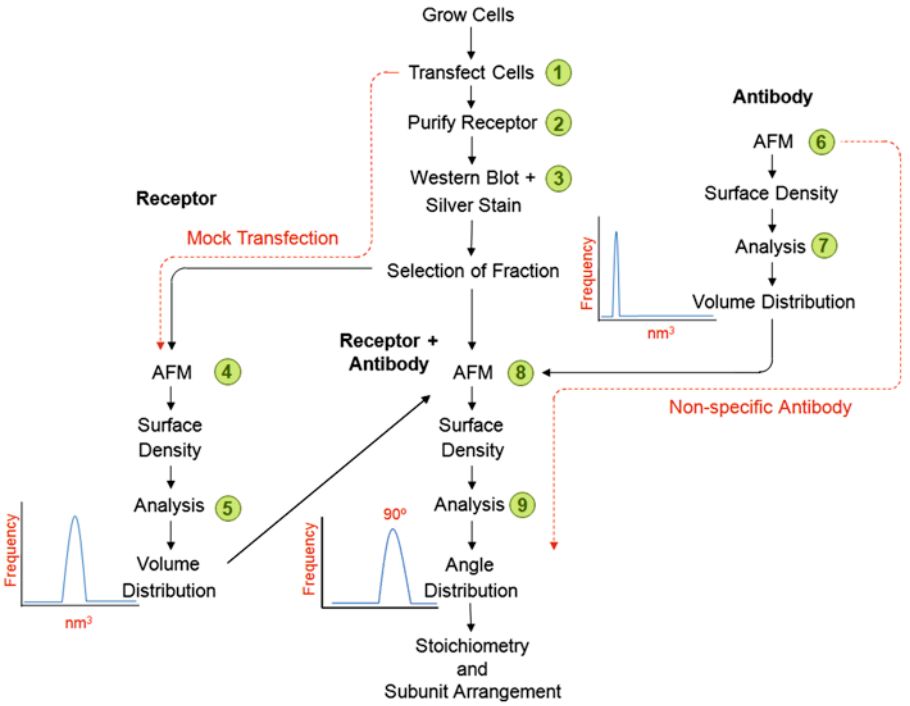

Fig. 2. Workflow of the AFM method to determine molecular architecture of receptors. The whole procedure consists of nine steps, as indicated in the illustration. *Steps 1–3* are associated with the purification process of the receptors. *Step 4* represents the AFM imaging of individual purified receptors in an adequate density for analysis. Usually, two controls are carried out for each experiment: (a) a mock transfection, and subsequent AFM imaging of the same elution fraction; (b) a co-incubation of receptors with nonspecific antibodies. Analysis of the AFM images is done automatically using an in-house Matlab algorithm (*step 5*). The same imaging procedure is performed with commercial anti-IgG antibodies (*steps 6 and 7*). Once volume distributions of the receptors and antibodies have been calculated, AFM imaging of the complexes is performed on approximately 100–150 μm^2 of scanning area (*step 8*). Note that volumes of antibodies are usually much smaller than the volumes of the receptors. Volumes of receptor–antibody complexes consistent with the presence of one receptor and one or more antibodies bound are selected (*step 9*). Doubly decorated receptors are further analyzed to calculate the angle between their particle peaks. The figure indicates the decoration of a tetrameric receptor, and so angles show the expected separation of antibodies at 90°.

describes a step-by-step protocol for the membrane protein purification process, adsorption onto mica, and AFM imaging of an adequate number of receptor–antibody complexes. It is expected that a moderately skilled person with basic knowledge of AFM operation and biochemistry will be able to reproduce the method faithfully.

2. Materials

2.1. Stock Buffers

1. Lysis stock solution: filtered 10 mM Tris–HCl, pH 7.6.
2. HBS 10× stock solution: filtered 0.5 M HEPES, pH 7.6, and 1 M NaCl.

2.2. Working Solutions for Receptor Isolation

1. HBS/EDTA buffer: HBS 1× solution, 2 mM ethylenediaminetetraacetic acid disodium salt (EDTA).
2. Lysis buffer: lysis stock solution, 0.5 mM EDTA. For a 5 ml solution, add 1 mM phenylmethylsulfonyl fluoride (PMSF) and one-half protease inhibitor tablet.
3. Solubilization buffer: HBS 1× solution, 0.5 M NaCl, and 1% 3-[(3-cholamidopropyl)dimethylammonio]-1-propanesulfonate (CHAPS). For a 9 ml solution, add 1 mM PMSF and one protease inhibitor tablet.
4. Washing buffer: HBS 1× solution and 0.5% CHAPS.
5. Washing buffer/low imidazole: washing buffer, 100 mM imidazole, and 0.5% CHAPS.
6. Elution buffer: washing buffer, 500 mM imidazole, and 0.5% CHAPS.

All working solutions should be prepared ~1 h before use and kept on ice.

2.3. AFM and Accessories

1. An AFM equipped with a 120-μm J-scanner and a dry imaging cell (Veeco, Santa Barbara, CA, USA).
2. Silicon cantilevers with a drive frequency of ~300 kHz and a specified spring constant of 40 N/m (MikroMasch, Madrid, Spain).

3. Methods

3.1. Receptor Isolation

All procedures are carried out at 4°C.

1. Collect flasks containing transfected cells.
2. Discard medium.
3. Wash once with HBS/EDTA buffer (add it gently, swirl a little, and then discard by pipetting – avoid losing live cells).
4. The cells are then removed from the flasks by agitation (hitting the sides and base of the flasks, and squirting the HBS directly onto the cells, pipetting up and down to collect more) with 9 ml of the same buffer. Transfer the cells into a 50-ml tube.
5. Rinse the flasks with another 10 ml of the same buffer (to collect remaining cells) and transfer the content into another 50-ml tube.
6. The cells are pelleted by centrifugation at ~900×*g* for 7 min at 4°C.
7. Begin centrifuge's cooling program (to 4°C).
8. The pellets are resuspended in 5 ml of lysis buffer. Transfer 5 ml of lysis buffer into the first tube and mix thoroughly. Transfer this to the second tube and mix thoroughly.

9. Incubate on ice for 20 min.
10. Put the homogenizer on ice.
11. The cells are homogenized with 30 strokes of the homogenizer.
12. The homogenate is transferred to four tubes and centrifuged at 660 × *g* for 8 min at 4°C.
13. The supernatant is removed and divided equally between four tubes. The pellet can sometimes have a rather diffuse boundary with the supernatant, so to improve purity of the final product, leave a little supernatant behind to ensure that the pellet remains undisturbed.
14. Two further tubes are filled with 400 µl of the supernatant, taking 200 µl from each of the four tubes.
15. All six tubes are centrifuged again at 21,000 × *g* for 15 min at 4°C.
16. Remove the supernatant.
17. Freeze the pellet from one of the two tubes containing 400 µl – this will be the "membrane fraction" for the Western blot (Fig. 3).
18. The pellets of the remaining five tubes are solubilized in a total volume of 9 ml of solubilization buffer. Take 1 ml of solubilizing buffer and thoroughly resuspend a pellet, and add the suspension to a fresh tube.
19. Repeat the same for all the pellets and pool the suspensions.
20. Add the remaining solubilization buffer, mix by inversion, and incubate for 1 h at 4°C with gentle rotation.
21. The suspension is transferred to a fresh Beckman ultracentrifuge tube.

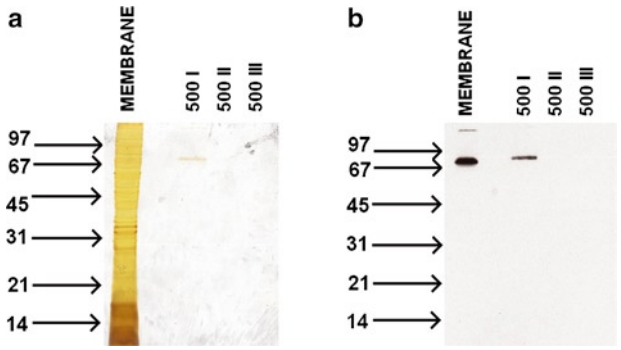

Fig. 3. Purification of membrane receptors containing His_6-tagged subunits, using nickel columns. This procedure corresponds to the *step 3* in the AFM method workflow shown in Fig. 2. (**a**) Silver staining of the membrane fraction showing a large number of solubilized proteins. After elution from the nickel column, only the first fraction with 500 mM imidazole gives a positive band for the His_6-tagged subunit. (**b**) Western blot using anti-His_6 antibody shows that the subunit is present in both the membrane fraction and the imidazole elution fraction.

22. Spin at 170,000 × *g* for 1 h at 4°C.
23. Start washing the beads 30 min before the spin is due to finish.
24. Cut the very end of a blue P1000 tip. Mix the beads (which will have settled) by inversion and transfer 1 ml of slurry into a fresh 15-ml tube.
25. Spin down (1,000 × *g* for 3 min).
26. Aspirate the supernatant, add 8 ml washing buffer, mix by inversion until all beads are resuspended, and spin down (1,000 × *g* for 3 min).
27. Repeat the previous step (2× washes in total).
28. Add the supernatant from the 170,000 × *g* spin (leaving roughly 0.5 ml behind to avoid disturbing the pellet) to the washed beads. Bring to 100 mM imidazole and incubate overnight at 4°C with gentle inversion.
29. On the next day, spin down the beads (1,000 × *g* for 3 min).
30. The beads are washed four times with 8 ml of washing buffer/low imidazole (as previously done – spin down, aspirate, and resuspend).
31. The beads are resuspended in an equal volume (~0.5 ml) of washing buffer and transferred to a purification column with a blue P1000 tip with the end cut off.
32. Wait a few minutes for the beads to settle, then break off the end of the column's cap.
33. Washing buffer eluent is allowed to run through into a beaker.
34. Prewash with 5 ml washing buffer/low imidazole.
35. Protein is eluted with 3 × 1 ml of elution buffer.
36. Western blot and silver staining protocol are carried out with the different fractions in order to detect which contains the greatest quantity of protein at the greatest purity (Fig. 3).

3.2. Adsorption of Purified Receptors onto Mica Support

1. Mica is cleaved to reveal pristine basal plane, which is then incubated with 1% poly-L-lysine for 30 min, washed under ultra-pure water, and dried under nitrogen.
2. Isolated receptors from the selected elution fraction are adsorbed onto poly-L-lysine-coated mica for 10 min (see Note 1), which is then washed 10× with 1 ml ultra-pure water and dried gently under dry nitrogen.

3.3. AFM Operation for the Imaging of Individual Receptors and Anti-tag Antibodies

1. For an appropriate AFM scan of an area of 1 μm^2 (see Note 2), not more than 50 isolated particles (receptors) should be observed, which in our experimental conditions corresponds to dilutions of the selected fraction in a range of 1:2 to 1:100 (see Note 3). Similarly, anti-tag antibodies previously absorbed

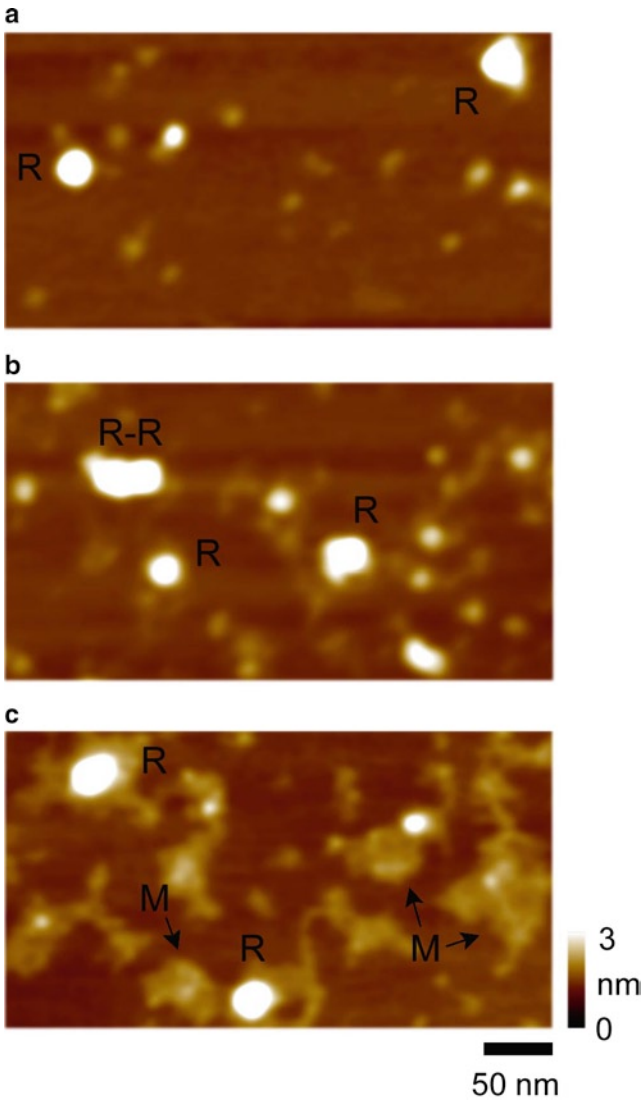

Fig. 4. Effect of sample preparation on the membrane protein adsorption onto mica. (**a**) Optimal density of adsorbed receptors (R) is observed after 10-min incubation on mica. More concentrated samples can generate either higher density with the presence of dimers of receptors (R–R) (**b**) or micelle-like structures (M) interacting with isolated receptors (**c**).

onto mica should be of a particle density of no more than 50–70 per 1 μm^2. The common AFM imaging parameters for air tapping mode are amplitude set point = 80–90% of free level, X/Y axis length = 1 μm, frequency of scanning = 3–4 Hz, integral gain = 0.25, proportional gain = 0.35, Z limit = 500–1,000 nm (see Notes 4 and 5), Z scale = 5–10 nm, and engage set point = 0.98–0.99 (Fig. 4a).

3.4. Co-incubation of Isolated Receptors and Anti-tag Antibodies In Vitro

1. Once optimal dilution conditions for the AFM imaging of individual receptors and antibodies are obtained, an overnight co-incubation of the components is carried out in vitro in a 1-ml Eppendorf tube at 4°C prior to deposition onto poly-L-lysine-coated mica. Depending upon the number and type of subunits within a receptor, it might be necessary to estimate the subunit orientation by decorating receptors with two antibodies at the same time. As IgG antibodies have similar molecular weights, one antibody should be cleaved by papain to generate Fab fragments, which are co-incubated with anti-tag IgG antibodies and purified receptors. Chemical modification of the mica surface with poly-glutamate or receptor ligands can also be used to force the adsorption of some domains. The application of Fab fragments and chemical modification is explained in detail in our paper on the characterization of the $\alpha_4\beta_3\delta$ $GABA_A$ receptor stoichiometry (6).

3.5. AFM Operation for the Imaging of Antibody–Receptor Complexes

1. Antibody–receptor complexes are imaged with AFM parameters similar to those used for the individual components (see Subheading 3.3 and Note 6). In order to perform an optimal identification of all the structures – free antibody and receptors, and complexes – the density of particles in an area of 1 μm^2 should not be above 100 (Fig. 5a).

3.6. Automatic Analysis of the Receptors and Complexes Using an In-House Algorithm and Interpretation of the Results

1. All the AFM images are analyzed using an in-house algorithm currently designed for Matlab language. Briefly, multiple thresholding is performed on the images in a stepwise decreasing manner to reduce the influence of the uneven mica surface due to poly-L-lysine or protein spreading.
2. Once geometric conditions are satisfied for each individual receptor, individual antibody, and antibody–receptor complex (formed when one, two, or more antibodies bind), segmentation in a probabilistic way is carried out on each structure. For each particle, parameters such as particle height (h) and half-height radii (r) are included in the equation of molecular volume $V_m = (\pi \times h/6)(3r^2 + h^2)$ (13). As a result, distributions of molecular volumes for all the components are automatically calculated. Each time a new antibody is used, a volume analysis of the isolated antibody should be carried out, as different IgGs, despite close similarities in molecular weight, can have different apparent molecular volumes.
3. Doubly decorated receptor–antibody complexes are further considered to calculate the angle distribution between the highest peaks of each protein (Fig. 5b, c). This information will give us the subunit orientation within a receptor. For example, a trimeric receptor should have adjacent bound

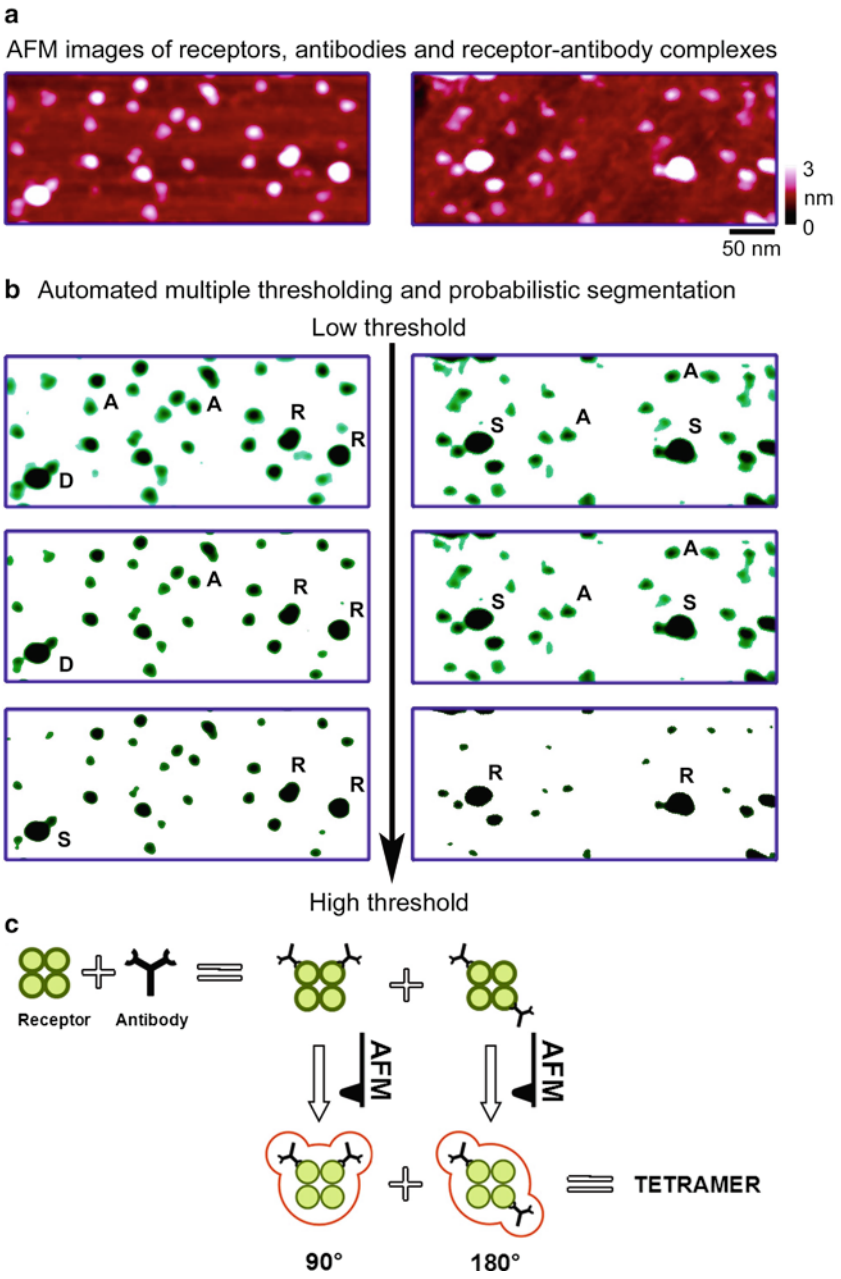

Fig. 5. Automated identification of tetrameric receptors, antibodies, and antibody–receptor complexes. (**a**) AFM images of receptors co-incubated with anti-subunit antibodies. (**b**) Multiple thresholding and segmentation of receptors (R), antibodies (A), and the following complexes: single antibody-bound receptors (S) and double antibody-bound receptors (D). It is observed that the optimal procedure allows positive identification of the different structures. A sequential increase in the thresholding values decreases the number of structures detected and makes artifacts such as (1) the S-complex generated from the correctly identified D-complex, and (2) the R generated from the correctly identified S-complex. (**c**) Scheme of the resulting interpretation derived from AFM imaging of the tetrameric receptor.

antibodies separated by an angle of 120°, and a tetramer by 90° and 180° (see Note 7). Depending upon the number of different subunits composing the receptor, a series of different anti-tag antibodies will be used. Note that a non-related anti-tag antibody should be tested to calculate unspecific binding profiles (Fig. 2). A full binding profile is then calculated for receptors co-incubated with several antibodies, which allows us to deduce the stoichiometry and orientation of subunits (details of the full automatic procedure are described in ref. 14).

4. Once a sufficient number of membrane protein complexes have been visualized by AFM, data acquisition and processing can be completed in approximately 10 min per 1 μm^2 scan (see Note 8).

3.7. Conclusion

We have presented here a detailed protocol for the AFM imaging of purified membrane receptors. We have demonstrated that the AFM imaging of receptor–anti-subunit antibody complexes can provide structural information about the subunit stoichiometry and orientation within a receptor. To our knowledge, apart from high-resolution techniques such as X-ray crystallography and EM, this is the only method that has been consistently applied to study the molecular architecture of membrane proteins, including receptors and ion channels. Therefore, we envisage its application to other families of membrane proteins including transporters, multiprotein enzymes, and molecular machines in the near future.

4. Notes

1. Timing of AFM sample deposition: We have demonstrated that the density of protein adsorbed onto mica does not change during 5–20 min after deposition (data not shown); therefore, as stated in our protocol, a period of 10 min is adequate to obtain enough individual receptors without producing overlapping of sample layers (Figs. 4a and 5a).
2. Capture of AFM images: When capturing consecutive images, ensure that the separation between images is double the width of the images being taken. For example, if capturing 1 µm × 1 µm images, a 1 µm separation between consecutive images will be insufficient, as the lateral positioning for most open-loop atomic force microscopes is such that a portion of the current image may overlap with a portion of the previous image, resulting in duplication of data for the regions imaged twice.

3. Adsorption of membrane proteins onto mica: Optimal density of adsorbed receptors is obtained by trial and error. If there is an excess of adsorbed receptors, unspecific aggregation of receptors can be observed (Fig. 4b). Similarly, a high concentration of detergent present on the mica can generate strong interactions with the isolated receptors (Fig. 4c).
4. *Z* limit: The Veeco Multimode AFM has 16-bit resolution on all three axes. This means that the data for each axis are expressed across ~66,000 divisions ($2^{16} = 65{,}536$). If the *Z* limit is set to maximum (~5.2 μm for a J-scanner), each division represents ~0.1 nm, which, when imaging objects, particularly antibodies that are often below 1 nm in height, can lead to significant pixellation on the vertical axis (Fig. 6a). Lowering the *Z* limit to 500 nm, or 10% of maximum, will decrease the size of each vertical division by a factor of 10, so that each division now represents 0.01 nm. This will not increase the vertical resolution fully tenfold, as 0.01 nm is near or most probably below the working vertical noise limit of most AFMs, but the reduction will reduce vertical pixellation and lead to more precise vertical measurements (Fig. 6b).
5. Automatic scanning: If using automatic scanning, approach the surface and image for ~30 min with the *Z* limit set to maximum, to allow the *Z*-piezo element to "settle." Once any

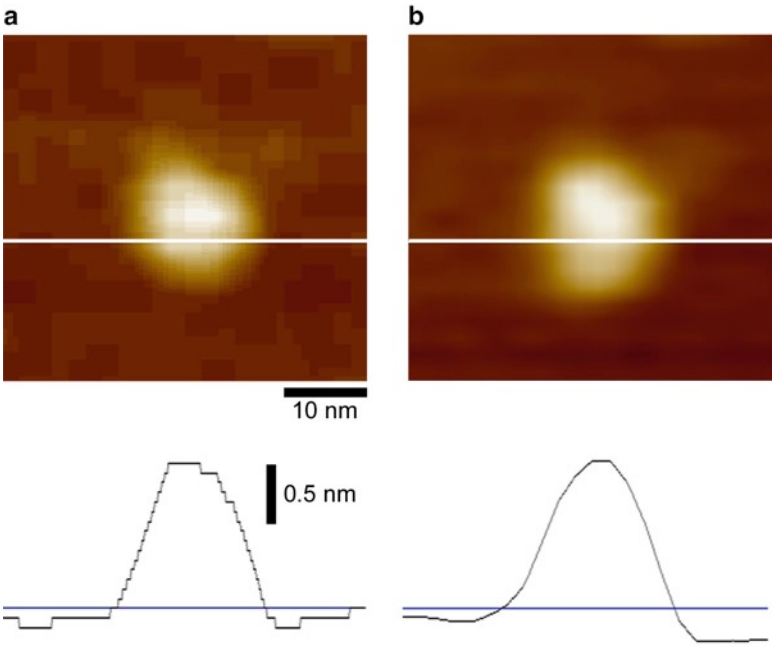

Fig. 6. Vertical pixellation effect on AFM imaging of antibodies. (**a**) *Z* limit set to 5.2 μm for the AFM imaging of an isolated IgG antibody. (**b**) *Z* limit set to 500 nm reduces vertical pixellation. Section analysis is indicated for both images.

drift has ceased, lower the *Z* limit to 500–1,000 nm and commence automated imaging. This is to prevent the *Z*-piezo from drifting out of its range due to drift.

6. Resolution of antibody–receptor complexes: The amplitude set point is kept at or above 80% of the free level to avoid excessive vertical compression of the sample. Furthermore, the selection of high engage set points (0.98–0.99) helps to preserve the geometry of the probe apex by helping to minimize the forces applied to it (and as a result also to the sample). Maximum resolution for scanning of membrane proteins has been achieved using contact mode AFM over ordered monolayers of proteins; however, the resolution is significantly lower for isolated membrane proteins (15). Although we usually use probes with stiff cantilevers (see Subheading 2.3, item 2) to ensure stable scanning of single membrane receptors, the instrument parameters mentioned above allows, in rare cases, high-resolution AFM images of receptors decorated with antibodies (Fig. 7).
7. Automatic identification of antibody–receptor complexes: Multiple thresholding values should be kept as low as possible to identify all the structures present on the surface. Although poly-L-lysine-coated mica is very flat, very small fluctuations in the surface will affect the thresholding values needed for receptor identification. A general suggestion is to keep this at 0.02 nm over the averaged height of surface fluctuations. Under higher thresholding values, some complexes and individual receptors may be absent from particle segmentation (Fig. 5b). In addition, this can lead to the incorrect identification of complexes, including the disappearance of antibodies

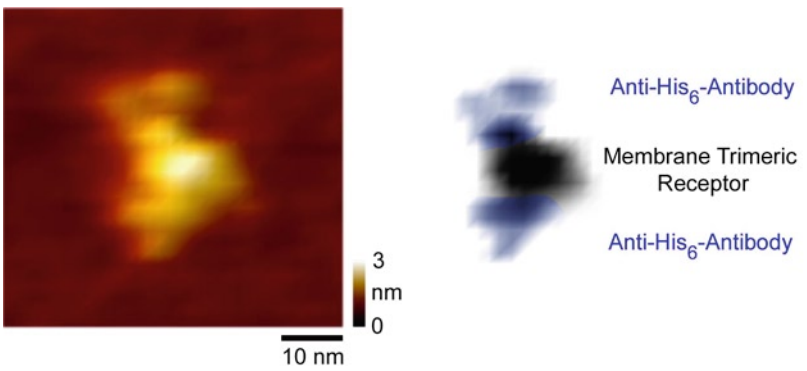

Fig. 7. High-resolution AFM image of the decoration of trimeric receptor. *Left panel* indicates an AFM image of a purified receptor complexed with anti-His_6 antibodies. *Right panel* shows the interpreted stoichiometry based on the image. Two IgG antibodies with the characteristic three domains (2 × Fab and Fc) are visible. Only one Fab domain interacts with the receptor. The angle between the highest peaks at every particle is around 120°, which suggests a trimeric stoichiometry for the receptor.

correctly bound to receptors (Fig. 5b). Note that calculated dimensions for each structure do not change under different thresholding. A scheme showing the final interpretation of the receptor stoichiometry is shown in Fig. 5c.

8. AFM scanning area: An area of 1 μm^2 is considered optimal for the automatic identification of receptor and antibody–receptor complexes. If an area bigger than 2 μm^2 is chosen, the frequency of scanning should be decreased up to 2 Hz to maintain stable tip–sample interaction. In addition, at a resolution of 512×512 pixels, selection of bigger scanning areas will result in a decrease in the number of complexes identified automatically. This low efficiency is due to the uncertainty of geometrical parameters associated with the multiple thresholding, which in turn prevents segmentation of complexes.

Acknowledgments

We thank Dr. Robert Henderson (Department of Pharmacology, University of Cambridge) and Drs. Haifang Ge and William Fitzgerald (Department of Engineering, University of Cambridge) for their support in AFM imaging and image processing.

References

1. Lacapere, J. J., Pebay-Peyroula, E., Neumann, J. M., and Etchebest, C. (2007) Determining membrane protein structures: still a challenge! *Trends Biochem Sci* **32**, 259–270.
2. Muller, D. J. (2008) AFM: a nanotool in membrane biology *Biochemistry* **47**, 7986–7998.
3. Shahin, V., and Barrera, N. P. (2008) Providing unique insight into cell biology via atomic force microscopy *Int Rev Cytol* **265**, 227–252.
4. Barrera, N. P., and Edwardson, J. M. (2008) The subunit arrangement and assembly of ionotropic receptors *Trends Neurosci* **31**, 569–576.
5. Barrera, N. P., Henderson, R. M., and Edwardson, J. M. (2008) Determination of the architecture of ionotropic receptors using AFM imaging *Pflugers Arch* **456**, 199–209.
6. Barrera, N. P., Betts, J., You, H., Henderson, R. M., Martin, I. L., Dunn, S. M., and Edwardson, J. M. (2008) Atomic force microscopy reveals the stoichiometry and subunit arrangement of the alpha4beta3delta GABA(A) receptor *Mol Pharmacol* **73**, 960–967.
7. Barrera, N. P., Henderson, R. M., Murrell-Lagnado, R. D., and Edwardson, J. M. (2007) The stoichiometry of P2X2/6 receptor heteromers depends on relative subunit expression levels *Biophys J* **93**, 505–512.
8. Barrera, N. P., Herbert, P., Henderson, R. M., Martin, I. L., and Edwardson, J. M. (2005) Atomic force microscopy reveals the stoichiometry and subunit arrangement of 5-HT3 receptors *Proc Natl Acad Sci USA* **102**, 12595–12600.
9. Barrera, N. P., Ormond, S. J., Henderson, R. M., Murrell-Lagnado, R. D., and Edwardson, J. M. (2005) Atomic force microscopy imaging demonstrates that P2X2 receptors are trimers but that P2X6 receptor subunits do not oligomerize *J Biol Chem* **280**, 10759–10765.
10. Barrera, N. P., Shaifta, Y., McFadzean, I., Ward, J. P., Henderson, R. M., and Edwardson, J. M. (2007) AFM imaging reveals the tetrameric structure of the TRPC1 channel *Biochem Biophys Res Commun* **358**, 1086–1090.
11. Carnally, S. M., Dev, H. S., Stewart, A. P., Barrera, N. P., Van Bemmelen, M. X., Schild, L., Henderson, R. M., and Edwardson, J. M. (2008) Direct visualization of the trimeric

structure of the ASIC1a channel, using AFM imaging *Biochem Biophys Res Commun* **372**, 752–755.

12. Ormond, S. J., Barrera, N. P., Qureshi, O. S., Henderson, R. M., Edwardson, J. M., and Murrell-Lagnado, R. D. (2006) An uncharged region within the N terminus of the P2X6 receptor inhibits its assembly and exit from the endoplasmic reticulum *Mol Pharmacol* **69**, 1692–1700.
13. Schneider, S. W., Lärmer, J., Henderson, R. M., and Oberleithner, H. (1998) Molecular weights of individual proteins correlate with molecular volumes measured by atomic force microscopy *Pflugers Arch* **435**, 362–367.
14. Barrera, N. P., Ge, H., Henderson, R. M., Fitzgerald, W. J., and Edwardson, J. M. (2008) Automated analysis of the architecture of receptors, imaged by atomic force microscopy *Micron* **39**, 101–110.
15. Fotiadis, D., and Engel, A. (2004) High-resolution imaging of bacteriorhodopsin by atomic force microscopy *Methods Mol Biol* **242**, 291–303.